Heliyon 10 (2024) e29649

Contents lists available at ScienceDirect

Heliyon

journal homepage: www.cell.com/heliyon

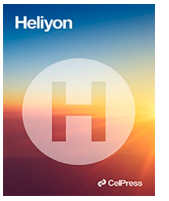

Research article

Phosphate recovery from aqueous phase using novel zirconium-based adsorbent

Yugo Uematsu [a], Fumihiko Ogata [a], Riko Okamoto [a], Mineaki Kabayama [b], Naohito Kawasaki [a,c,*]

[a] Faculty of Pharmacy, Kindai University, 3–4–1, Kowakae, Higashi–Osaka, Osaka, 577–8502, Japan
[b] BIRCH Lab., 214, Akinokamikamihonjyou, Seto–cho, Naruto, Tokushima, 771-0360, Japan
[c] Antiaging Center, Kindai University, 3–4–1 Kowakae, Higashi–Osaka, Osaka, 577-8502, Japan

ARTICLE INFO

Keywords:
Phosphate ion
Zirconium
Adsorption

ABSTRACT

This study aims to document the phosphate ion (PO_4^{3-}) adsorption capacity of a novel zirconium-based adsorbent. The physicochemical properties of the adsorbent are investigated using an array of methods and metrics such as electron microscopy, X-ray diffraction, thermal analysis, specific surface area, pore volume, pH point of zero charge (pH_{pzc}), and surface hydroxyl groups. The batch method is used to elucidate PO_4^{3-} adsorption capacity. Results suggested that the adsorption of PO_4^{3-} was based on an internal diffusion and a monolayer adsorption. We also clarified that the pH of the solution significantly impacted the adsorption. Moreover, the adsorbent shows the ability to not only adsorb but also desorb PO_4^{3-} for at least five cycles, based on an adsorption mechanism that we document. These findings indicate that this adsorbent could serve as a major industrial PO_4^{3-} adsorbent.

1. Introduction

Phosphorus is used pervasively in modern society, such as in fertilizers and detergents, and it is expected that global phosphorus demand will continue to increase as the global population continues to rise [1,2]. However, in countries such as Japan, almost all phosphorus must be imported because there is no domestic phosphorus resource [3]. Recently, the prospect of global exhaustion of phosphorus resources has aroused substantial fear [4]. Therefore, an urgent problem is to build systems of phosphorus recovery and reuse. At the same time, phosphorus that is not recycled but rather leaked into the environment, primarily as aqueous PO_4^{3-}, acts as a pollutant by inducing eutrophication [5]. Hence, removal of surplus phosphorus from the aqueous environment is a vital task from multiple perspectives. Building PO_4^{3-} recovery systems will contribute not only to the recycling of finite phosphorus resources, but also to the improvement of the aqueous environment.

PO_4^{3-} recovery systems operating via several methods have been reported in previous studies [6–8]. Particularly, adsorption method is used widely because it is simple and it can be carried out effectively at small scales. Various types of adsorbents (e.g. steel slag, clay minerals, and polyglutamic acid) have been indicated to be useful PO_4^{3-} adsorbents so far [9–11]. Activated carbon is one of the most famous adsorbents for various adsorbate, and PO_4^{3-} is no exception. Many types of activated carbon had been investigated the

* Corresponding author. Laboratory of Public Health, Faculty of Pharmacy, Kindai University, 3–4–1, Kowakae, Higashi–Osaka, Osaka, 577–8502, Japan.
E-mail address: kawasaki@phar.kindai.ac.jp (N. Kawasaki).

https://doi.org/10.1016/j.heliyon.2024.e29649
Received 2 October 2023; Received in revised form 1 April 2024; Accepted 11 April 2024
Available online 14 April 2024

abilities of PO_4^{3-} adsorption [12,13]. However, Bacelo et al. [14] said activated carbon usually had a negative charge and it was not suitable to adsorb anionic adsorbate such as PO_4^{3-}. In recent, a new type of activated carbon for PO_4^{3-} adsorption, modified by metal and its compounds (such as lanthanum, pyrolusite and Zr–Al type double hydroxide), have been reported [15–17]. In other words, it is considered that the existence of metal such as aluminum (Al) and zirconium (Zr) in adsorbents is one of the most important factors to adsorb PO_4^{3-}. Our previous studies have also reported that various metal hydroxides had excellent PO_4^{3-} adsorption capacity [18–21]. Among these metal complex hydroxide materials, zirconium hydroxide particularly shows high selectivity for PO_4^{3-} [22]. Chitrakar et al. [23] reported that zirconium(IV) oxide exhibited a capacity for PO_4^{3-} adsorption from seawater more than thrice those of oxides of Fe, Al, and Mn. Moreover, Zr has very little toxicity and high stability [24], making it ideal for PO_4^{3-} recovery applications. However, only a few reports have studied the PO_4^{3-} adsorption capacity of Zr compounds. In the present study, we created a novel adsorbent with Zr (Novel Zr compound: NZC) to adsorb PO_4^{3-} more efficiently and investigated its properties. Moreover, we also elucidated the PO_4^{3-} adsorption capacity of NZC and evaluated its performance under repeated adsorption–desorption cycles.

2. Materials and methods

2.1. Materials

NZC was provided by the BIRCH Lab (Tokushima, Japan). The NZC was prepared by the following procedures. In briefly, 0.42 mol/L zirconium oxychloride solution and 1.7 mol/L sodium carbonate solution were mixed, and subsequently heated at 100 °C for 15 min. After reaction, the residue was washed with distilled water and dried at 100 °C for 9 h. The particle size of obtained NZC was <500 μm. Standard reagents zirconium(IV) hydroxide ($Zr(OH)_4$) and zirconium(IV) oxide (ZrO_2) were obtained from Sigma-Aldrich Japan G.K. (Tokyo, Japan) and FUJIFILM Wako Pure Chemical Co. (Osaka, Japan), respectively. The test solution including PO_4^{3-} was prepared using potassium dihydrogen phosphate (KH_2PO_4, FUJIFILM Wako Pure Chemical Co., Osaka, Japan).

Surface morphology was measured using an SU1510 unit (Hitachi High-Technology). Crystallinity was measured using a MiniFlex II unit (Rigaku). Elemental analysis was performed using a JXA-8530F unit (JEOL). Binding energy was measured using an AXIS-NOVA unit (Shimadzu). Thermal analysis was performed using a TG8120 unit (Rigaku). Specific surface areas and pore volumes were analyzed using a NOVA 4200*e* unit (Yuasa Ionics). The evaluations of pH_{pzc} [25] and hydroxyl group surface density were carried out using methods drawn from previous studies [26,27].

2.2. Adsorption kinetics study of PO_4^{3-} using NZC

A total of 0.05 g of NZC was added to 50 mL of PO_4^{3-} test solution at a concentration of 153.4 mg/L (i.e., 50 mg phosphorus per liter). Each such mixture was shaken at 100 rpm at 25 °C for a period lasting between 1 and 24 h. After shaking, the solution was filtered with a 0.45-μm membrane filter. The absorbance of filtrate was analyzed at a wavelength of 610 nm using a DR/890 absorption spectrometer (HACH, USA). The amount of PO_4^{3-} adsorbed was calculated according to

$$q_a = (C_0 - C_e)V/W \quad (1)$$

Where q_a is the amount of PO_4^{3-} adsorbed (mg/g); C_0 and C_e are the initial and the equilibrium concentration of PO_4^{3-} (mg/L), respectively; V is the volume of test solution (L); and W is the weight of NZC (g). The data were reported as mean ± standard error (*S.E.*).

2.3. Adsorption isotherms of PO_4^{3-} using NZC

PO_4^{3-} test solutions with concentrations ranging from 3.1 to 153.4 mg/L (i.e., from 1 to 50 mg phosphorus per liter) were prepared. A total of 0.05 g of NZC was added to 50 mL of each solution. Each mixture was shaken at 100 rpm for 24 h at a temperature of 7 °C, 25 °C, or 45 °C. After shaking, each solution was filtered using a 0.45-μm membrane filter, and the filtrate was analyzed using the DR/890 absorption spectrometer. The amount of PO_4^{3-} adsorbed was calculated using Eq. (1), and the data were reported as mean ± *S.E.*

2.4. Effect of solution pH for the adsorption of PO_4^{3-} using NZC

PO_4^{3-} test solutions with a concentration of 153.4 mg/L (i.e., 50 mg phosphorus per liter) was prepared, and the pH of each solution was adjusted to a value between 2 and 12. A total of 0.05 g of NZC was added to 50 mL of each solution, and each mixture was shaken at 100 rpm at 25 °C for 24 h. After shaking, each solution was filtered with a 0.45-μm membrane filter, and the filtrate was analyzed using the DR/890 absorption spectrometer. The amount of PO_4^{3-} adsorbed was calculated using Eq. (1), and the data were reported as mean ± *S.E.*

2.5. Effect of the coexistence anion for the adsorption of PO_4^{3-} using NZC

Test solutions were prepared, each including 153.4 mg/L of PO_4^{3-} and 153.4 mg/L of one of the coexistence anions; chloride (Cl^-), sulfate (SO_4^{2-}), or nitrate (NO_3^-). 0.05 g of NZC was added to 50 mL of each complex solution. Each mixture was shaken at 100 rpm at 25 °C for 24 h. After shaking, each solution was filtered with a 0.45-μm membrane filter. PO_4^{3-} and other coexistence anions in the

filtrate were analyzed using the DR/890 absorption spectrometer and a Dionex ICS-900 ion chromatograph (Thermo Fisher Scientific Inc., Japan). The ion chromatography conditions were as follows. The mobile phase was 2.7 mmoL/L sodium carbonate +0.3 mmol/L sodium bicarbonate. The regenerant was 12.5 mmol/L sulfuric acid. The flow rate was 1.5 mL/min. The sample volume was 10 μL. Elution times under the experimental conditions were 2.1 min for Cl^-, 10.7 min for SO_4^{2-}, and 7.1 min for NO_3^-. The amount adsorbed in each case was calculated using Eq. (1), and all data were reported as mean ± *S.E.*

2.6. Adsorption and desorption study of PO_4^{3-} using NZC

A total of 0.9 g of NZC was added to 900 mL of a PO_4^{3-} test solution with a concentration of 153.4 mg/L (i.e., 50 mg phosphorus per liter). The mixture was shaken at 100 rpm at 25 °C for 24 h. After shaking, each solution was filtered with a 0.45-μm membrane filter. The filtrate was analyzed using the DR/890 absorption spectrometer, and the amount of PO_4^{3-} adsorbed was calculated using Eq. (1). All post-filtration residues were completely dried at 50 °C.

The desorption process was carried out as follows. Sodium hydroxide (NaOH) solutions were prepared at concentrations of 1, 10, 100, and 1000 mmol/L 0.05 g of residue was added to 50 mL of each solution. Each mixture was shaken at 100 rpm at 25 °C for 24 h. After shaking, each solution was filtered with a 0.45-μm membrane filter. Each filtrate was analyzed using the DR/890 absorption spectrometer. The amount of PO_4^{3-} desorbed and the desorption rate in each case were calculated using Eq. (2) and Eq. (3), respectively. Equations are shown as

$$q_d = VC_e/W \tag{2}$$

$$R_d = q_d/q_e \times 100 \tag{3}$$

Where, q_d and q_e are the amount of PO_4^{3-} desorbed and adsorbed (mg/g), respectively; R_d is the desorption rate (%); V is the volume of test solution (L); and W is the weight of NZC (g). All data were reported as mean ± *S.E.*

3. Results and discussion

3.1. Properties of adsorbents

Fig. S1 shows the morphological properties of NZC and the standard reagents $Zr(OH)_4$ and ZrO_2. The scanning electron microscopy image (Fig. S1(a)) of NZC was broadly similar to that of $Zr(OH)_4$. The X-ray diffraction pattern of NZC in Fig. S1(b) showed no sharp peaks, and the pattern was more similar to that of $Zr(OH)_4$ than that of ZrO_2. These findings together suggest an amorphous structure for NZC.

The thermal analysis of NZC is shown in Fig. 1. These results show that the thermogravimetric (TG) curve of NZC decreased between 100 °C and 200 °C and was flat beyond approximately 200 °C. The final residual rate of NZC after analysis was 74.7 %. Differential thermal analysis (DTA) peaks indicated that an endothermic reaction occurred at around 100 °C and an exothermic reaction occurred around 400 °C. Together, these TG and DTA peaks and thermal analysis results enable estimation of which reaction(s) occurred at each temperature. We interpret the TG and DTA peaks between 100 °C and 200 °C as representing a dehydration reaction eliminating moisture adhering to NZC. Alternatively, the exothermal reaction at around 400 °C suggests an NZC crystallization reaction. This interpretation is similar to those reported for $Zr(OH)_4$ and $ZrO(OH)_2$ in a previous study [28,29]. Theoretically, both $Zr(OH)_4$ and $ZrO(OH)_2$ undergo calcination reactions to yield ZrO_2 via the following reaction formulas:

$$Zr(OH)_4 \rightarrow ZrO_2 + 2H_2O$$

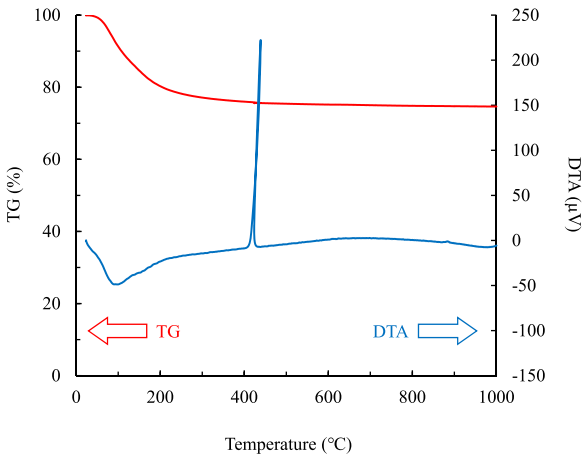

Fig. 1. Thermal analysis of NZC under an air atmosphere.

$ZrO(OH)_2 \rightarrow ZrO_2 + H_2O$

The residual rates of the above reactions are approximately 67 % and 84 %, respectively. Based on these results, we considered NZC likely to consist of a mixture of $Zr(OH)_4$ and $ZrO(OH)_2$. In this study, we did not analyze the FT-IR spectrum of NZC because we considered that it was not to need for discussion of this study. However, it can be deduced that NZC's FT-IR spectrum could be similar to the one in the previous study [29]. At a moment, detailed of components of NZC have not be fully clarified this compositional question and we have to investigate more detail as a future issue to investigate.

The physicochemical properties of NZC are shown in Table S1. NZC exhibited a high specific surface area (234.3 m^2/g) but had low numbers of surface hydroxyl groups (0.78 mmol/g). NZC exhibited various types of pores. In the International Union of Pure and Applied Chemistry classification of pore types by diameter, micropore diameters are less than 2 nm, mesopore diameters are between 2 and 50 nm, and macropore diameters are greater than 50 nm [30]. In this framework, NZC exhibited primarily mesopores (18.9 cc/g) rather than micropores (4.27 cc/g) or macropores (1.24 cc/g). As reported in Table S1, the pH_{pzc} of NZC was 4.0. Generally, the adsorbent acquires a positive charge when solution pH < pH_{pzc} condition because the adsorbent behaves as an acid by adsorbing OH^-. Conversely, in solution pH > pH_{pzc} condition, the adsorbent acquires a negative charge because the adsorbent behaves as a base by adsorbing H^+ [31,32]. With these results as a starting point, we elucidated the detailed properties of the novel adsorbent NZC.

3.2. Adsorption kinetics study of PO_4^{3-} using NZC

Fig. S2 shows the PO_4^{3-} adsorption kinetics of NZC. Equilibrium PO_4^{3-} adsorption was reached within 18–24 h after shaking began. The equilibrium amount of PO_4^{3-} adsorbed at 24 h was 38.1 mg/g.

Many aqueous-phase adsorption reactions can be fitted to one of two kinetics models: a pseudo-first-order model (PFOM) or a pseudo-second-order model (PSOM). The linear equations representing PFOM and PSOM can be shown in Eq. (4) and Eq. (5), respectively [33,34].

$$\ln (q_{e,exp} - q_t) = \ln q_{e,cal} - k_1 t \quad (4)$$

$$t/q_t = t/q_{e,cal} + 1/(k_2 \cdot q_{e,cal}^2) \quad (5)$$

Where, $q_{e,exp}$ and $q_{e,cal}$ are the maximum amounts of PO_4^{3-} adsorbed (mg/g) according to the experiment and calculation, respectively; q_t is the amount adsorbed (mg/g) at any time t (h); and k_1 and k_2 are constants for PFOM (1/h) and PSOM (g/mg/h), respectively. The experimental data for an adsorption reaction with a surface adsorption mechanism are expected to be well fitted by PFOM, while those for an adsorption reaction with an internal diffusion mechanism are expected to be well fitted by PSOM [35,36].

Table 1 provides the results of these model fittings. For NZC the correlation coefficients of PFOM and PSOM were found to be approximately equal. However, the experimental $q_{e,cal}$ value was closer to that of PSOM than that of PFOM. This observation suggests an internal diffusion mechanism for the adsorption of PO_4^{3-} onto NZC.

3.3. Adsorption isotherms of PO_4^{3-} using NZC

Fig. S3 shows PO_4^{3-} adsorption isotherms of NZC. The amount of PO_4^{3-} adsorbed tended to increase as the temperature increased. In general, aqueous-phase adsorption isotherms can be fitted to one of two popular models: the Langmuir isotherm model and the Freundlich isotherm model [37,38]. The linear equations representing these two isotherm models can be shown in Eq. (6) and Eq. (7), respectively

$$1/q = 1/q_{max} + 1/(K_L q_{max} C) \quad (6)$$

$$\log q = \log K_F + (1/n) \log C \quad (7)$$

Where, q is the amount of PO_4^{3-} adsorbed (mg/g), C is the equilibrium concentration (mg/L), q_{max} is the maximum amount adsorbed as calculated from the Langmuir isotherm model (mg/g), K_L is the Langmuir constant (L/mg), and K_F and $1/n$ are the dimensionless constants of the Freundlich isotherm model. The value of $1/n$ indicates the difficulty of adsorption by the adsorbent; $1/n$ values between 0.1 and 0.5 indicate good adsorptive capacity, whereas $1/n$ values exceeding 2 indicate poor adsorptive capacity [39].

Table 2 shows the Langmuir and Freundlich constants derived from our experiments. In every condition, the correlation coefficient of Langmuir isotherm model was higher than the one of Freundlich isotherm model. These results suggested that adsorption isotherms in this study were well fitted by Langmuir isotherm model, with monolayer adsorption as the mechanism for NZC's PO_4^{3-} adsorption. In results of the Freundlich isotherm constants, the $1/n$ value ranged from 0.68 to 0.39, which suggested that NZC is a moderately good PO_4^{3-} adsorbent.

Table 1
Parameters of adsorption kinetics for the adsorption of PO_4^{3-}.

Adsorbents	$q_{e,exp}$ (mg/g)	Pseudo-first-order model			Pseudo-second-order model		
		k_1 (1/h)	$q_{e,cal}$ (mg/g)	r	k_2 (g/mg/h)	$q_{e,cal}$ (mg/g)	r
NZC	38.1	0.13	30.7	0.989	6.0 × 10−3	42.9	0.989

Table 2
Langmuir and Freundlich isotherm constants for the adsorption of PO_4^{3-}.

Adsorbents	Temperature (°C)	Langmuir isotherm model			Freundlich isotherm model		
		q_{max}(mg/g)	K_L (L/mg)	r	1/n	K_F	r
NZC	7 °C	47.1	0.03	0.997	0.68	1.44	0.978
	25 °C	26.8	2.69	0.976	0.39	5.06	0.840
	45 °C	34.8	1.37	0.989	0.42	5.85	0.822

3.4. Surface analyses of NZC before and after PO_4^{3-} adsorption

Fig. 2(a) provides a qualitative analysis of the NZC surface, while Fig. 2(b) shows the binding energy of NZC surface. In Fig. 2(a), the intensity of phosphorus increased from 20 before adsorption to 48 after adsorption. Moreover, in Fig. 2(b)–a phosphorus-derived peak around 130 eV was detected in the graph only after adsorption. These results confirm the presence of PO_4^{3-} on the NZC surface after adsorption.

3.5. Effect of solution pH on the PO_4^{3-} adsorption capacity of NZC

Fig. 3 shows the amount of PO_4^{3-} adsorbed by NZC at various solution pH conditions. As a result, the amount of PO_4^{3-} adsorbed was significantly enhanced under pH 2−3 conditions and decreased with pH 4−7 situations. Conversely, under basic conditions (pH ≥ 8), the amount of PO_4^{3-} decreased more notably. These findings can be explained by phosphoric acid dissociation behavior.

Phosphoric acid has three pK_a points (pK_{a1} = 2.1, pK_{a2} = 7.2, and pK_{a3} = 12.7). The valence of the phosphate ion changes with pH conditions. In acidic conditions, phosphoric acid exists as the molecular form H_3PO_4 or dissociates into the monovalent ionic form $H_2PO_4^-$; with increasing solution pH, the acid dissociates further to HPO_4^{2-} and then to PO_4^{3-}. On the other hand, according to the pH_{pzc} data, NZC exists as a cationic form at pH < 4 but in an anionic form at pH > 4 [40]. Therefore, we consider the ionic attraction between negatively charged $H_2PO_4^-$ and positively charged NZC in acidic conditions to be responsible for inducing such voluminous PO_4^{3-} adsorption. These results demonstrate that key factors determining NZC adsorption of phosphate included the pH-induced charge on NZC and the identity of the phosphorus-bearing ion in the aqueous phase.

3.6. Effect of coexistence anions on the adsorption of PO_4^{3-} using NZC

In real-world aqueous environments, many anions co-occur with PO_4^{3-}. For this reason, the PO_4^{3-} adsorption selectivity of NZC was evaluated by examining the effect of coexistence anions on PO_4^{3-} adsorption by NZC. In particular, Cl^-, SO_4^{2-}, and NO_3^- were used as coexistence anions. Fig. 4 shows the amounts of PO_4^{3-} adsorbed by NZC in the presence of each of these anions. The presence of Cl^- barely affected the amount of PO_4^{3-} adsorbed. In contrast, the presence of SO_4^{2-} or NO_3^- caused PO_4^{3-} adsorption to be lower than in

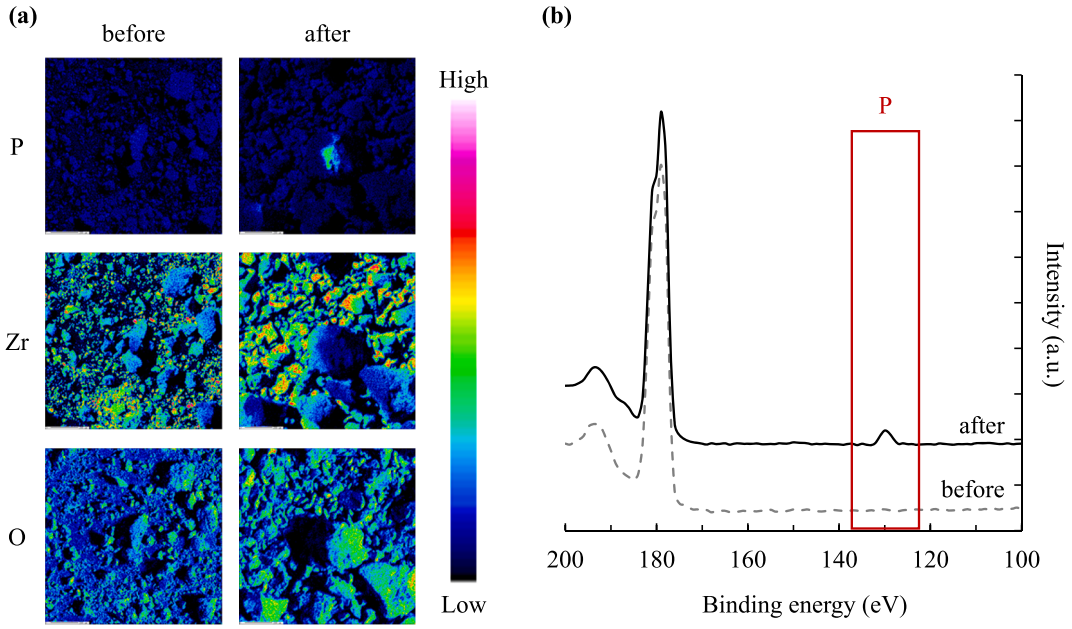

Fig. 2. Surface analysis of NZC before and after PO_4^{3-} adsorbed (a): Quantitative analysis, (b): Binding energy.

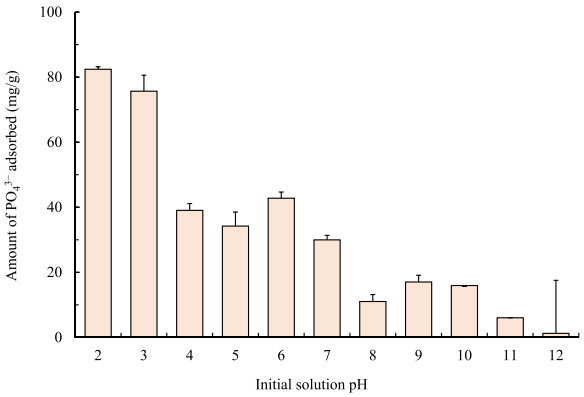

Fig. 3. Amount of PO_4^{3-} adsorbed onto NZC at different pH Initial concentration: 153.4 mg/L, pH in solution: 2–12, solvent volume: 50 mL, adsorbent: 0.05 g, contact time: 24 h, temperature: 25 °C, agitation speed: 100 rpm.

their absence. We also evaluated amounts of each anion adsorbed onto NZC under same conditions. As a result, Cl^- and NO_3^- were not adsorbed onto NZC but SO_4^{2-} was adsorbed onto NZC (approximately 3.4 mg/g).

PO_4^{3-} and SO_4^{2-} have almost the same ionic radius (2.12 Å and 2.19 Å, respectively), and under certain pH conditions their dissociation products have the same ion valence [40]. Moreover, these anions have different structures; the tetrahedral structure (PO_4^{3-} and SO_4^{2-}) and the plane triangle structure (NO_3^-), respectively. These similarities explain why SO_4^{2-} most strongly affected PO_4^{3-} adsorption by NZC. However, the decrease in the amount of PO_4^{3-} adsorption by NZC associated with the presence of other anions was not substantial. These observations suggest that NZC may exhibit high selectivity of adsorption with respect to PO_4^{3-} in the presence of many other anions occupying the aqueous environment. In addition, we also have to investigate the detail effect NO_3^- on PO_4^{3-} adsorption with NZC in the future.

3.7. Adsorption and desorption studies of PO_4^{3-} using NZC

Phosphorus, especially in the form of PO_4^{3-}, is a key planetary resource. Therefore, a desirable PO_4^{3-} adsorbent is one that excels not only at adsorbing but also desorbing PO_4^{3-} for reuse, to the benefit of society and the planet. In the results reported above, we found that NZC could not adsorb PO_4^{3-} under alkaline conditions. Consequently, NZC has the inherent potential to desorb PO_4^{3-} under alkaline conditions. Hence, we investigated the possibility of PO_4^{3-} desorption by NZC in solutions with various concentrations of NaOH, with results as shown in Fig. 5. The amount of PO_4^{3-} desorbed from NZC was greater in solutions with higher concentrations of NaOH. These results suggest that NZC adsorbed PO_4^{3-} under acidic conditions and released it under alkaline conditions.

Continuing in this motivation, we considered NZC's ability to repeatedly adsorb and desorb PO_4^{3-}. Fig. 6 depicts the amounts of PO_4^{3-} adsorbed and desorbed up to five cycles. From cycle 2 onward, amounts adsorbed and desorbed decreased substantially compared to those in cycle 1. Alternatively, cycles 2–5 yielded roughly constant results in terms of not only the amounts of PO_4^{3-} adsorbed and desorbed but also the desorption rate. Results suggested that there were two types of PO_4^{3-} adsorption site on NZC: desorbable sites and un-desorbable sites. In other words, it was considered that PO_4^{3-} adsorption by NZC might occur via a combination

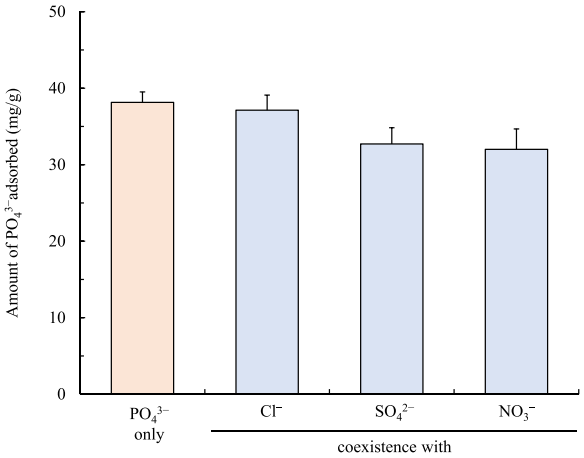

Fig. 4. Amount of PO_4^{3-} adsorbed under the coexistence with other anions Initial concentration: 153.4 mg/L, solvent volume: 50 mL, adsorbent: 0.05 g, contact time: 24 h, temperature: 25 °C, agitation speed: 100 rpm.

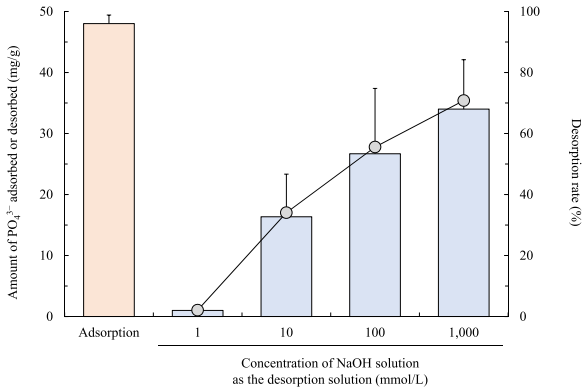

Fig. 5. Amount of PO_4^{3-} adsorbed and desorbed onto NZC. ■: amount adsorbed, □: amount desorbed, ○: desorption rate. (Adsorption) Initial concentration of PO_4^{3-}: 153.4 mg/L, solvent volume: 900 mL, adsorbent: 0.9 g, contact time: 24 h, temperature: 25 °C, agitation speed: 100 rpm. (Desorption) Initial concentration of NaOH: 1−1000 mmol/L, solvent volume: 50 mL, adsorbent: 0.05 g, contact time: 24 h, temperature: 25 °C, agitation speed: 100 rpm.

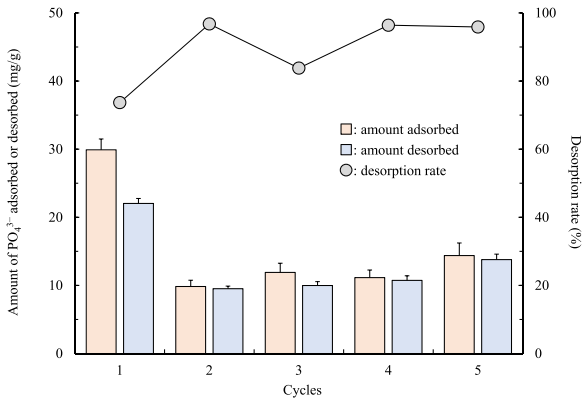

Fig. 6. Repeatedly adsorption and desorption of PO_4^{3-} using NZC. ■: amount adsorbed, □: amount desorbed, ○: desorption rate. (Adsorption) Initial concentration of PO_4^{3-}: 153.4 mg/L, solvent volume: 500 mL, adsorbent: 0.5 g (cycle 1), whole amount (cycle 2−5), contact time: 24 h, temperature: 25 °C, agitation speed: 100 rpm. (Desorption) Initial concentration of NaOH: 1000 mmol/L, solvent volume: 500 mL, adsorbent: whole amount, contact time: 24 h, temperature: 25 °C, agitation speed: 100 rpm.

of two different adsorption mechanisms: a reversible mechanism and an irreversible mechanism. However, at the moment, the detail mechanism of PO_4^{3-} adsorption onto NZC hasn't been elucidated yet. Therefore, we have to continue investigating the adsorption capacity of NZC to PO_4^{3-}.

4. Conclusion

We investigated PO_4^{3-} adsorption by a NZC in aqueous phase. Measurable properties indicated that NZC may be a mixture of Zr $(OH)_4$ and $ZrO(OH)_2$. NZC achieved PO_4^{3-} adsorption equilibrium within 18–24 h, likely via an adsorption mechanism of internal diffusion. Isotherms of PO_4^{3-} adsorption by NZC indicated that monolayer adsorption was involved. NZC adsorbed PO_4^{3-} especially well at low pH and showed high selectivity of PO_4^{3-} adsorption even in the presence of several other anions. Various factors affected NZC's PO_4^{3-} absorbance, including the pH-induced charge on NZC and the identity of the phosphorus-bearing ion in the aqueous phase. Furthermore, NZC successfully repeatedly adsorbed and desorbed PO_4^{3-} in response to changes in pH conditions. In conclusion, NZC, a novel Zr-based adsorbent, shows great potential as a PO_4^{3-} adsorbent. This study paves the way for further advances in phosphorus recycling technology.

Data availability statement

Data included in article/supplementary material/referenced in article.

CRediT authorship contribution statement

Yugo Uematsu: Writing – review & editing, Writing – original draft, Investigation, Formal analysis, Data curation, Conceptualization. **Fumihiko Ogata:** Writing – review & editing, Writing – original draft, Project administration, Investigation, Conceptualization. **Riko Okamoto:** Writing – original draft, Visualization, Investigation, Formal analysis. **Mineaki Kabayama:** Writing – original draft, Resources, Investigation. **Naohito Kawasaki:** Writing – original draft, Supervision, Project administration.

Declaration of competing interest

The authors declare that they have no known competing financial interests or personal relationships that could have appeared to influence the work reported in this paper.

Appendix A. Supplementary data

Supplementary data to this article can be found online at https://doi.org/10.1016/j.heliyon.2024.e29649.

References

[1] D. Cordell, J.-O. Drangert, S. White, The story of phosphorus: global food security and food for thought, Glob, Environ. Change 19 (2) (2009) 292–305, https://doi.org/10.1016/j.gloenvcha.2008.10.009.
[2] I.W. Almanassra, G. Mckay, V. Kochkodan, M.A. Atieh, T. Al-Ansari, A state of the art review on phosphate removal from water by biochars, J. Chem. Eng. 409 (1) (2021) 128211, https://doi.org/10.1016/j.cej.2020.128211.
[3] S. Sugiyama, K. Wakisaka, K. Imanishi, M. Kurashina, N. Shimoda, M. Katoh, et al., Recovery of phosphate rock equivalents from incineration ash of chicken manure by elution-precipitation treatment, J. Chem. Eng. Jpn. 52 (9) (2019) 778–782, https://doi.org/10.1252/jcej.19we030.
[4] L. Shu, P. Schneider, V. Jegatheesan, J. Johnson, An economic evaluation of phosphorus recovery as struvite from digester supernatant, Bioresour. Technol. 97 (17) (2006) 2211–2216, https://doi.org/10.1016/j.biortech.2005.11.005.
[5] D.L. Correll, The role of phosphorus in the eutrophication of receiving waters: a review, J. Environ. Qual. 27 (2) (1998) 261–266, https://doi.org/10.2134/jeq1998.00472425002700020004x.
[6] Y. Shimizu, I. Hirasawa, Recovery of ionic substances from wastewater by seeded reaction crystallization, Chem. Eng. Technol. 35 (6) (2012) 1051–1054, https://doi.org/10.1002/ceat.201100647.
[7] Y. Dai, Y. Li, Y. Ke, B. Li, Efficiency and mechanism of advanced treatment for phosphate wastewater by high efficiency and low consumption coagulation and phosphorus removal system, IOP Conf. Ser. Earth Environ. Sci. 631 (2021) 012002, https://doi.org/10.1088/1755-1315/631/1/012002.
[8] Z. Yuan, S. Pratt, D.J. Batstone, Phosphorus recovery from wastewater through microbial processes, Curr. Opin. Biotechnol. 23 (6) (2012) 878–883, https://doi.org/10.1016/j.copbio.2012.08.001.
[9] C. Shi, X. Wang, S. Zhou, X. Zuo, C. Wang, Mechanism, application, influencing factors and environmental benefit assessment of steel slag in removing pollutants from water: a review, J. Water Process Eng. 47 (2022) 102666, https://doi.org/10.1016/j.jwpe.2022.102666.
[10] F. Long, J.-L. Gong, G.-M. Zeng, L. Chen, X.-Y. Wang, J.-H. Deng, et al., Removal of phosphate from aqueous solution by magnetic Fe–Zr binary oxide, Chem. Eng. J. 171 (2) (2011) 448–455, https://doi.org/10.1016/j.cej.2011.03.102.
[11] L. Han, Y. Wang, W. Zhao, H. Zhang, F. Guo, T. Wang, et al., Cost-effective and eco-friendly superadsorbent derived from natural calcium-rich clay for ultra-efficient phosphate removal in diverse waters, Sep. Purif. Technol. 297 (2022) 121516, https://doi.org/10.1016/j.seppur.2022.121516.
[12] A.K. Ouakouak, L. Youcef, Phosphates removal by activated carbon, Sens. Lett. 14 (6) (2016) 600–605, https://doi.org/10.1166/sl.2016.3664.
[13] K. Boki, S. Tanada, T. Miyoshi, R. Yamasaki, N. Ohtani, T. Tamura, Phosphate removal by adsorption to activated carbon, Jpn. J. Hyg. 42 (3) (1987) 710–720, https://doi.org/10.1265/jjh.42.710.
[14] H. Bacelo, A.M.A. Pintor, S.C.R. Santos, R.A.R. Boaventura, C.M.S. Botelho, Performance and prospects of different adsorbents for phosphorus uptake and recovery from water, Chem. Eng. J. 381 (2020) 122566, https://doi.org/10.1016/j.cej.2019.122566.
[15] P.T. Huong, K. Jitae, B.L. Giang, T.D. Nguyen, P.Q. Thang, Novel lanthanum-modified activated carbon derived from pine cone biomass as ecofriendly biosorbent for removal of phosphate and nitrate in wastewater, Rend. Fis. Acc. Lincei 30 (2019) 637–647, https://doi.org/10.1007/s12210-019-00827-3.
[16] S. Yao, M. Wang, J. Liu, S. Tang, H. Chen, T. Guo, et al., Removal of phosphate from aqueous solution by sewage sludge-based activated carbon loaded with pyrolusite, J. Water Reuse Desalination 8 (2) (2018) 192–201, https://doi.org/10.2166/wrd.2017.054.
[17] P. Karthikeyan, S. Meenakshi, Synthesis and characterization of Zn–Al LDHs/activated carbon composite and its adsorption properties for phosphate and nitrate ions in aqueous medium, J. Mol. Lq. 296 (2019) 111766, https://doi.org/10.1016/j.molliq.2019.111766.
[18] F. Ogata, D. Imai, M. Toba, M. Otani, N. Kawasaki, Properties of novel adsorption produced by calcination of nickel hydroxide and its capability for phosphate ion adsorption, J. Ind. Eng. Chem. 34 (2016) 172–179, https://doi.org/10.1016/j.jiec.2015.11.005.
[19] F. Ogata, N. Nagai, M. Kishida, T. Nakamura, N. Kawasaki, Interaction between phosphate ions and Fe-Mg type hydrotalcite for purification of wastewater, J. Environ. Chem. Eng. 7 (1) (2019) 102897, https://doi.org/10.1016/j.jece.2019.102897.
[20] F. Ogata, S. Iijima, M. Toda, M. Otani, T. Nakamura, N. Kawasaki, Characterization and phosphate adsorption capability of novel nickel-aluminum-zirconium complex hydroxide, Chem. Pharm. Bull. 68 (3) (2020) 292–297, https://doi.org/10.1248/cpb.c19-01053.
[21] F. Ogata, E. Ueta, M. Toda, M. Otani, N. Kawasaki, Adsorption of phosphate ions from an aqueous solution by calcined nickel-cobalt binary hydroxide, Water Sci. Technol. 75 (1−2) (2017) 94–105, https://doi.org/10.2166/wst.2016.492.
[22] Q. Zhang, Q. Du, T. Jiao, B. Pan, Z. Zhang, Q. Sun, et al., Selective removal of phosphate in waters using a novel of cation adsorbent: zirconium phosphate (ZrP) behavior and mechanism, Chem. Eng. J. 221 (2013) 315–321, https://doi.org/10.1016/j.cej.2013.02.001.
[23] R. Chitrakar, S. Tezuka, A. Sonoda, K. Sakane, K. Ooi, T. Hirotsu, Selective adsorption of phosphate from seawater and wastewater by amorphous zirconium hydroxide, J. Colloid Interface Sci. 297 (2) (2006) 426–433, https://doi.org/10.1016/j.jcis.2005.11.011.
[24] J. Lin, Y. Zhan, H. Wang, M. Chu, C. Wang, Y. He, et al., Effect of calcium ion on phosphate adsorption onto hydrous zirconium oxide, Chem. Eng. J. 309 (2017) 118–129, https://doi.org/10.1016/j.cej.2016.10.001.
[25] E.N. Bakatula, D. Richard, C.M. Neculita, G.J. Zagury, Determination of point of zero charge of natural organic materials, Environ. Sci. Pollut. Res. 25 (2018) 7823–7833, https://doi.org/10.1007/s11356-017-1115-7.
[26] P.C.C. Faria, J.J.M. Orfao, M.F.R. Pereira, Adsorption of anionic and cationic dyes on activated carbons with different surface chemistries, Water Res. 38 (8) (2004) 2043–2052, https://doi.org/10.1016/j.watres.2004.01.034.
[27] H. Yamashita, Y. Ozawa, F. Nakajima, T. Murata, Ion exchange properties and uranium adsorption of hydrous titanium(IV) oxide, J. Chem. Soc. Japan. 1978 (8) (1978) 1057–1061, https://doi.org/10.1246/nikkashi.1978.1057.

[28] G.-Y. Guo, Y.-L. Chen, W.-J. Ying, Thermal, spectroscopic and X-ray diffractional analyses of zirconium hydroxides precipitated at low pH values, Mater. Chem. Phys. 84 (2−3) (2004) 308–314, https://doi.org/10.1016/j.matchemphys.2003.10.006.
[29] T. Sato, The thermal decomposition of zirconium oxyhydroxide, J. Therm. Anal. Calorim. 69 (2002) 255–265, https://doi.org/10.1023/A:1019962428910.
[30] B.D. Zdravkov, J.J. Čermák, M. Šefara, J. Janků, Pore classification in the characterization of porous materials: a perspective, Cent. Eur. J. Chem. 5 (2007) 385–395, https://doi.org/10.2478/s11532-007-0017-9.
[31] Y. Uematsu, F. Ogata, N. Nagai, C. Saenjum, T. Nakamura, N. Kawasaki, In vitro removal of paraquat and diquat from aqueous media using raw and calcined basil seed, Heliyon 7 (7) (2021) e07644, https://doi.org/10.1016/j.heliyon.2021.e07644.
[32] J.-W. Shim, S.-J. Park, S.-K. Ryu, Effect of modification with HNO_3 and NaOH on metal adsorption by pitch-based activated carbon fibers, Carbon 39 (11) (2001) 1635–1642, https://doi.org/10.1016/S0008-6223(00)00290-6.
[33] S. Lagergren, Zur theorie der sogenannten adsorption gelöster stoffe, K. - Sven. Vetenskapsakademiens Handl. 24 (1898) 1–39.
[34] Y.S. Ho, G. McKay, Pseudo-second order model for sorption processes, Process Biochem. 34 (5) (1999) 451–465, https://doi.org/10.1016/S0032-9592(98)00112-5.
[35] T. Ishizaka, A. Kawashima, Experimental evaluations of sampling rate for passive air sampler, J. Environ. Chem. 26 (4) (2016) 203–210, https://doi.org/10.5985/jec.26.203.
[36] W.-Y. Huang, R.-H. Zhu, F. He, D. Li, Y. Zhu, Y.-M. Zhang, Enhanced phosphate removal from aqueous solution by ferric-modified laterites: equilibrium, kinetics and thermodynamic studies, Chem. Eng. J. 228 (2013) 679–687, https://doi.org/10.1016/j.cej.2013.05.036.
[37] I. Langmuir, The constitution and fundamental properties of solids and liquids, J. Am. Chem. Soc. 38 (11) (1916) 2221–2295, https://doi.org/10.1021/ja02268a002.
[38] H.M.F. Freundlich, Over the adsorption in solution, J. Phys. Chem. 57 (1906) 385–471.
[39] S. Tsukinoki, K. Yamada, O. Itoh, N. Nanbu, Y. Akama, Solid phase extraction of Cu, Ni and Co by EDTA type chelating cellulose, Bunseki Kagaku 57 (12) (2008) 1033–1038, https://doi.org/10.2116/bunsekikagaku.57.1033.
[40] R.D. Shannnon, Revised effective ionic radii and systematic studies of interatomic distances in halides and chalcogenides, Acta Crystallogr. A32 (5) (1976) 751–767, https://doi.org/10.1107/S0567739476001551.